Article

pubs.acs.org/Biomac

Photoinitiated Alkyne–Azide Click and Radical Cross-Linking Reactions for the Patterning of PEG Hydrogels

Rodney T. Chen,[†,‡] Silvia Marchesan,[‡] Richard A. Evans,[‡] Katie E. Styan,[‡] Georgina K. Such,[†] Almar Postma,[†,‡] Keith M. McLean,[‡] Benjamin W. Muir,*[,‡] and Frank Caruso[†]

[†]Department of Chemical and Biomolecular Engineering, The University of Melbourne, Parkville, Victoria, 3010, Australia

[‡]CSIRO Materials Science and Engineering, Bayview Avenue, Clayton, Victoria, 3168, Australia

Supporting Information

ABSTRACT: The photolithographical patterning of hydrogels based solely on the surface immobilization and cross-linking of alkyne-functionalized poly(ethylene glycol) (PEG-tetraalkyne) is described. Photogenerated radicals as well as UV absorption by a copper chelating ligand result in the photochemical redox reduction of Cu(II) to Cu(I). This catalyzes the alkyne–azide click reaction to graft the hydrogels onto an azide-functionalized plasma polymer (N_3PP) film. The photogenerated radicals were also able to abstract hydrogen atoms from PEG-tetraalkyne to form poly(α-alkoxy) radicals. These radicals can initiate cross-linking by addition to the alkynes and intermolecular recombination to form the PEG hydrogels. Spatially controlling the two photoinitiated reactions by UV exposure through a photomask leads to surface patterned hydrogels, with thicknesses that were tunable from tens to several hundreds of nanometers. The patterned PEG hydrogels (ca. 60 μm wide lines) were capable of resisting the attachment of L929 mouse fibroblast cells, resulting in surfaces with spatially controlled cell attachment. The patterned hydrogel surface also demonstrated spatially resolved chemical functionality, as postsynthetic modification of the hydrogels was successfully carried out with azide-functionalized fluorescent dyes via subsequent alkyne–azide click reactions.

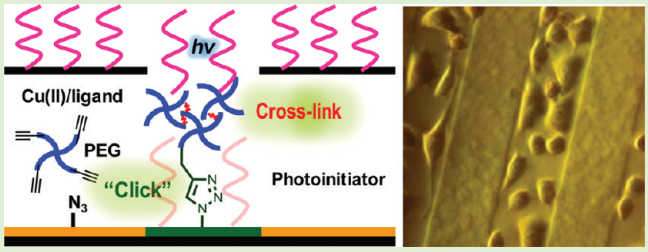

INTRODUCTION

Surface modification to reduce biofouling is of great interest in numerous applications, ranging from biosensors to biomedical implants and devices.[1] Poly(ethylene glycol) (PEG) is well-known to impart protein as well as cell and bacteria-resistant properties to surfaces.[2] There are a number of well-established methods for the surface coating of PEG. These include the use of self-assembled monolayers (SAMs)[3] and polymer brushes.[4] More recently, research has focused on the surface patterning of PEG polymer films and microstructures that allow the precise spatial control of surface properties for bioactive and responsive biomaterials applications.[5]

There is a variety of microfabrication techniques for the surface patterning of PEG, including microcontact printing (μCP),[6] capillary force lithography (CFL),[7] molecular assembly patterning by lift-off (MAPL),[8] and asymmetric glow discharge plasma polymerization.[9] Another technique suitable for generating polymer patterns is photolithography. Photoirradiation through a photomask leads to spatial and temporal control over photopolymerization, photocross-linking and functionalization reactions.[10] Many reports on the photolithographical fabrication and patterning of PEG hydrogels have been based on free-radical photopolymerization of diacrylate PEG derivatives.[11]

Recently, the photoinitiation of the copper-catalyzed alkyne–azide cycloaddition (CuAAC) click reaction has been demonstrated.[12] Prior to this, the alkyne–azide click reaction lacked the spatial and temporal control associated with photoinitiated processes.[13] This development coincides with an increasing interest in bioorthogonal click reactions that are initiated by light, namely, "photoclick" chemistry. These include photoinitiated thiol-ene,[14] thiol-yne,[15] alkene–tetrazole cycloaddition,[16] and Diels-Alder reactions.[17]

In this study, we describe a versatile approach for the micropatterning of hydrogels based upon the coupling of alkyne-functionalized PEG (PEG-tetraalkyne) to an azide-functionalized bromine plasma polymer (N_3PP) film. The alkyne–azide click reaction covalently grafts the PEG macromers onto the N_3PP film, which is catalyzed by the photochemical reduction of Cu(II) to Cu(I) via photoinitiator radicals[12] and light absorption by a copper-chelating ligand.[18] The hydrogen-donating character of PEG[19] also allows the photoinitiator radicals to induce radical cross-linking of the macromer via radical addition to the alkynes as well as intermolecular recombination to form PEG hydrogels. Controlling the two photoinitiated reactions through a photomask leads to hydrogels with well-resolved spatial patterning. The patterned hydrogels exhibited tunable thick-

Received: December 17, 2011
Revised: January 26, 2012
Published: February 14, 2012

nesses, resistance to cell attachment and reactivity toward further chemical modification. We also highlight the importance of using an effective Cu(I) chelating ligand for high yielding photopatterned hydrogels. To the best of our knowledge, this is the first example of the production of patterned hydrogels based solely upon the cross-linking[20] of alkyne-functionalized PEG. One attractive aspect of this method compared to other reports on the patterning of PEG hydrogels from diacrylates,[11] is that the hydrogels are reactive to further CuAAC reactions, which is an effective strategy for the chemoselective immobilization of biomolecules.

EXPERIMENTAL SECTION

General/Materials. PEG tetraalkyne (MW = 10 and 20 kDa, Creative PEGworks, U.S.A.), Alexa Fluor (AF) 488 alkyne (Invitrogen), and Alexa Fluor 647 azide (Invitrogen), Irgacure 2959 (I2959; BASF), copper(II) sulfate pentahydrate ($CuSO_4{\cdot}5H_2O$, BDH, 99%), potassium carbonate (Aldrich, 99%), sodium ascorbate, ethylenediaminetetracetic acid (EDTA, BDH, 98%), 3-butyn-2-ol (Aldrich, 97%), and tetraethyleneglycol dimethyl ether (Acros, 99%) were used without purification. High purity Milli-Q water (MQ-water) with a resistivity greater than 18 MΩ cm was obtained from an inline Millipore RiOs/Origin system. The preparation of bromine and azide-functionalized plasma polymer surfaces[21a] and the synthesis of the carboxylated TBTA ligand (**L**)[22a] have been previously reported.

Preparation of PEG Hydrogels by Photoinitiated Cross-Linking. A polymer precursor solution, containing PEG-tetraalkyne (30% w/w) with potassium carbonate (35 mM) and equal concentrations of $CuSO_4{\cdot}5H_2O$, Irgacure 2959, and ligand (**L**; 9 mM) was prepared in MQ-water. The mixture was briefly sonicated to ensure complete dissolution. The solution was pipetted (ca. 30 μL) onto a glass slide and spread to fill an area of diameter about 1.5 cm and thickness about 300 μm. The solution was irradiated with an EXFO Acticure 4000 UV/vis spot cure system, with a 250−450 nm bandpass filter and a light intensity of 100 mW/cm^2 for 1 h. The hydrogel was removed and hydrated in MQ-water (1 mL) and then freeze-dried overnight.

Preparation of Patterned and Surface Immobilized PEG Hydrogels. A polymer precursor solution was prepared in identical proportions as above, except that the polymer concentration was 10% w/w. The solution was spin-casted onto azide-functionalized bromine plasma polymer (N_3PP) coated silicon wafers (11 mm^2) using a Laurell WS400B-6NPP spin coater. A drop of the solution (20 μL) was placed in the center of the surface and carefully spread out with a glass slide. The substrate was then spun at speeds of 750 rpm for 30 s and then 8400 rpm for 60 s, with ramp-up times of 10 and 15 s, respectively, before being placed in a custom-built UV irradiation box, where a chrome photomask on a quartz plate (Bandwidth Foundry, Australia) was placed on top. The mask was weighed down by two metal discs (ca. 115 g each) placed on either side of the substrate to ensure intimate contact with the mask and the spin-cast film. The sample was irradiated with UV light from an EXFO Acticure 4000 UV/vis spot cure system, with a 250−450 nm bandpass filter and an intensity of 35 mW/cm^2 for 250, 500, and 900 s. The substrates were subsequently immersed in MQ-water and 0.1 M EDTA for approximately 30 min each and finally rinsed with copious amounts of MQ-water to develop the pattern.

Postfunctionalization of Patterned PEG Hydrogels with Click Dyes. Patterned PEG hydrogels were first immersed in EDTA solution (0.1 M) overnight to ensure removal of copper. Solutions of sodium ascorbate (500 μL, 6 mM, in MQ water), AF-647 azide (1 μL, 0.5 mg/mL, in DMSO), and $CuSO_4{\cdot}5H_2O$ (500 μL, 2 mM, in MQ water) were added to the patterned substrates. The reaction was allowed to proceed for 18 h, at room temperature, in the dark with slight agitation (60 rpm) after which the surfaces were rinsed with copious amounts of MQ water. Subsequently, the masked N_3PP regions were fluorescently labeled in a similar fashion with AF-488 alkyne. Control reactions were prepared without the addition of $CuSO_4{\cdot}5H_2O$ to the hydrogel.

L929 Mouse Fibroblast Cell Attachment Assay. Patterned samples were sterilized by immersion in 2X Anti-Anti (antibiotic−antimycotic, GIBCO) solution for at least 60 min, and then rinsed once with media (MEM + GlutaMAX-I, GIBCO), supplemented with 10% v/v FBS (fetal bovine serum, SAFC Biosciences), 1% v/v NEAA (nonessential amino acids, GIBCO), and 1% v/v Anti-Anti. L929 mouse fibroblasts were trypsinized (Tryple Express, Invitrogen), rinsed by centrifugation (240 g for 5 min), and resuspended in media (100000 cells/mL). The membrane dye DilC12(3) (BD Biosciences, 10 μg/mL) was added and the cell suspension and was incubated at 37 °C in a 5% CO_2/air atmosphere for 60 min, after which excess DilC12(3) was removed by rinsing the cells three times in media (240 g for 5 min). Cells were placed in the wells of a 12-well plate (Nunc) containing the patterned samples, at a concentration of 25000 cells/cm^2 of well area in media (1.2 mL), and incubated overnight at 37 °C with 5% CO_2/air atmosphere. Nonadherent cells were removed by rinsing the samples in fresh media. Cell viability was investigated using an esterase activity assay. Cells were incubated in the medium described above but with only 2% v/v FBS in the presence of Calcein AM (2 μM, Invitrogen) for 30 min.

Characterization Methods. Dynamic time sweep rheological analysis was conducted on an Ares photorheometer (TA Instruments, U.S.A.) with a 20 mm quartz parallel plate geometry and a Peltier temperature control unit. An EXFO Acticure 4000 UV/vis spot cure system was connected via a liquid light-guide. A 30% w/w polymer precursor solution was prepared exactly as above and dispensed (75 μL) between the quartz plates. The temperature and gap were set at 25 °C and 10 μm, respectively, along with UV light at 250−450 nm with an intensity of 100 mW/cm^2. A constant strain of 10% and a frequency of 7 rad/s were used. Postpolymerization strain sweeps showed strains of 3 to 15% to be in the linear region at the applied frequency. Likewise, postpolymerization frequency sweeps showed frequencies of 4 to 15 rad/s to be in the linear region at the applied strain.

Fluorescence images of fluorescently labeled hydrogels were visualized using a confocal laser-scanning microscope (TCS SP2; Leica, Germany). Fluorescence images of adherent cells on patterned samples were imaged on an inverted microscope (Nikon Eclipse TE2000-U). DilC12(3) was excited at 510−560 nm, with the resulting emission above 590 nm, while for Calcein excitation occurred at 450−490 nm and the resulting emission above 520 nm was observed.

MAS (magic angle spinning) ^{13}C NMR of the freeze-dried hydrogel was performed on a Bruker BioSpin Av500 at 500.13 MHz with a MAS BBO broad-band probe. The hydrogel was loaded into 4 mm ZrO_2 cylindrical rotors and spun at a spinning rate of 4.5 kHz. Solution ^1H and ^{13}C NMR were performed on a Bruker Av400H at 400.13 kHz.

Raman spectroscopy analysis was performed on a Renishaw Invia confocal micro-Raman spectrometer operating at a laser wavelength of 514.5 nm. Measurements were taken at full power with acquisition times of 20 s.

Atomic force microscopy images of patterned hydrogels (dehydrated) were analyzed with an Asylum Research MFP-3D atomic force microscope, using ultrasharp silicon nitride tips (NSC 15 noncontact silicon cantilevers, MikroMasch) in tapping mode. All measurements were made at room temperature.

Scanning force microscopy analysis was carried out using Philips FEG SEM XL30S, with an accelerating voltage of 2 eV. Samples were coated with a thin film of iridium (ca. 2 Å) prior to imaging.

X-ray photoelectron spectroscopy (XPS) analysis was performed in an AXIS HSi spectrometer (Kratos Analytical Ltd., U.K.) equipped with a monochromated Al Kα X-ray source at a power of 144 W (12 mA, 12 kV). Peak assignments were determined from the measured binding energy values, which were charge-corrected with respect to the main aliphatic hydrocarbon peak, which was set at 285 and 286.5 eV for the ethylene oxide peak.[23]

RESULTS AND DISCUSSION

Study of PEG Hydrogel Cross-Linking. In this study, we employed a photoinitiator, Irgacure 2959 (4-(2-hydroxyethoxy)phenyl-(2-hydroxy-2-propyl)ketone), and a

water-soluble carboxylated version of the commonly used copper-chelating click ligand, tris[(1-benzyl-*H*-1,2,3-triazol-4-yl)methyl]amine (**L**; Figure 1D).[20] The photochemical redox

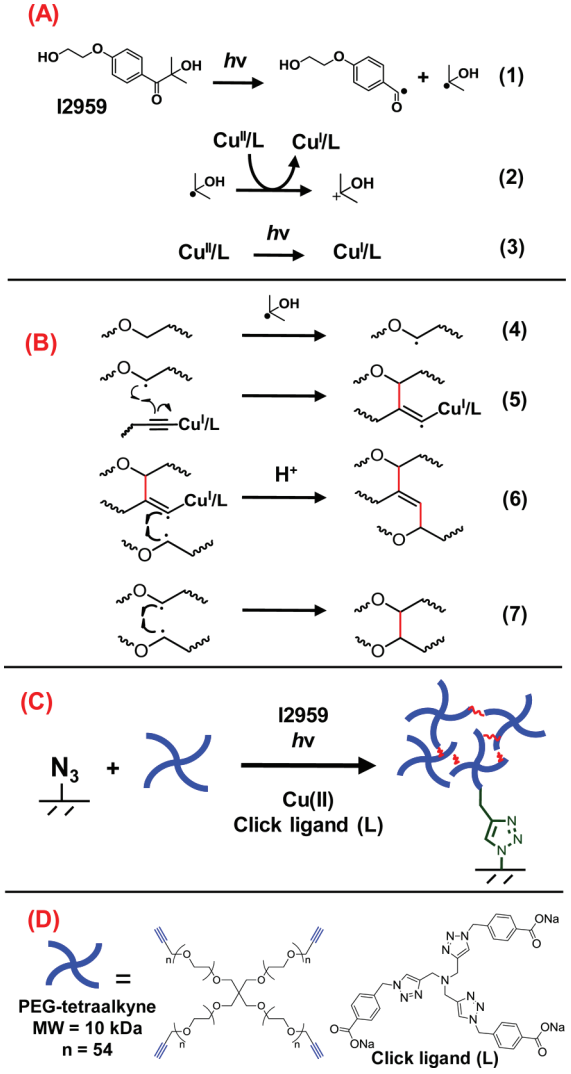

Figure 1. (A) Redox reduction of Cu(II) to Cu(I) via photoinitiator radicals and the UV absorption by the click ligand; (B) Proposed mechanisms for radical cross-linking of PEG-tetraalkyne; (C) General scheme for photoinitiated alkyne–azide click and radical-cross-linking reactions of PEG hydrogel on an azide-functionalized surface; (D) Chemical structures of the PEG-tetraalkyne and click ligand (**L**).

reduction of Cu(II) to transiently generate Cu(I) was achieved in two ways: the photogeneration of radicals via the photoinitiator[12a] (**2**) and the absorption of UV light by the ligand[18] (**3**), which promotes the intramolecular electron transfer from the π-system of the ligand to the chelated Cu(II) ion (Figure 1A).[18] The ligand also stabilizes and simplifies the Cu(I) reactions by allowing it to occur under ambient conditions while enhancing Cu(I) catalytic activity.[24] An aqueous solution of four-arm PEG-tetraalkyne, the photoinitiator, Cu(II), and the ligand (**L**) was irradiated with UV light to form PEG hydrogels. In addition to generating Cu(I), the photoinitiator radicals are likely to abstract labile PEG α-hydrogens to form poly(α-alkoxy) radicals (**4**; Figure 1B),[19] which undergo intermolecular recombination to form vinyl radicals (**5**) through addition to the nucleophilic vinylidene-like β-carbon of the Cu–acetylide complex.[25] The vinyl radicals can then add to poly(α-alkoxy) radicals to form ether cross-links (**6**). Ether cross-links can also occur through the recombination between two poly(α-alkoxy) radicals (**7**).[19] This proposed mechanism was supported by both Raman spectroscopy and magic-angle spinning (MAS) ^{13}C NMR analysis. The Raman spectra of both the PEG-tetraalkyne macromer and the PEG hydrogel showed a small peak at about 2100 cm^{-1}, which corresponds to the C≡C acetylenic stretch (Figure 2). For the

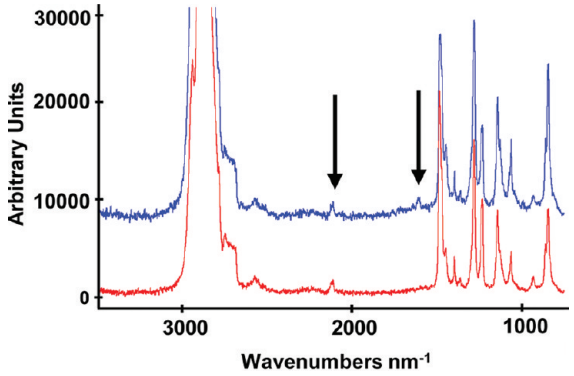

Figure 2. Raman spectra of PEG hydrogel (blue line) and PEG-tetraalkyne (red line) with arrows corresponding to peaks at 2113 (C≡C stretch) and 1611 cm^{-1} (C=C stretch). Hydrogel synthesized in the presence of Cu(I), ligand (**L**), and Irgacure 2959 with 250–450 nm UV light.

PEG hydrogel, a small peak occurs at about 1611 cm^{-1}, which corresponds to substituted alkenes. ^{13}C NMR analysis of the PEG-tetraalkyne macromer reveals resonances at 79.3 and 76 ppm that correspond to C≡C carbons (Figure 3a). MAS ^{13}C NMR analysis of the PEG hydrogel shows a broadening of the peak at 69.5 ppm, corresponding to ethylene oxide (ether) carbons and small peaks at 109.4 and 130.1 ppm, which again correspond to substituted alkenes (Figure 3b). Aromatic or hydroxyl signals arising from the photoinitiator and ligand were not observed. PEG cross-linking and alkene formation were further confirmed by ^{1}H NMR studies on water-soluble, small molecules as model compounds with separate alkyne and ether functionalities (see Supporting Information, Figure S1). Dynamic time sweep rheological analyses were conducted to monitor gelation during the photoinitiated cross-linking of PEG-tetraalkyne. Complete gelation occurred after about 17.5 min, with the gel point ($G' > G''$ and 10 Pa) occurring at about 13.5 min (Figure 4). In the presence of the photoinitiator, but without Cu(I) and the ligand (**L**), the gelation kinetics were slower with a gel point at about 26.5 min. This difference in kinetics is due to the nucleophilic activation of the alkynes arising from the Cu–ligand (**L**) complex.[26] The consumption of the photoinitiator, Irgacure 2959, during photoirradiation was monitored by UV–vis spectroscopy. Aqueous solutions of the photoinitiator with identical concentrations as the photorheology experiments were separately irradiated with the same light conditions. Even at the strongest irradiation conditions (100 mW, 30 min), there is still strong absorbance occurring at about 280 nm (Figure 5). Thus, this indicates that the photoinitiator has not been fully consumed before the occurrence of gelation in the photorheology studies. It also supports the contribution of UV absorption by the copper-chelating ligand in transiently generating Cu(I) species.

dx.doi.org/10.1021/bm201802w | *Biomacromolecules* 2012, 13, 889–895

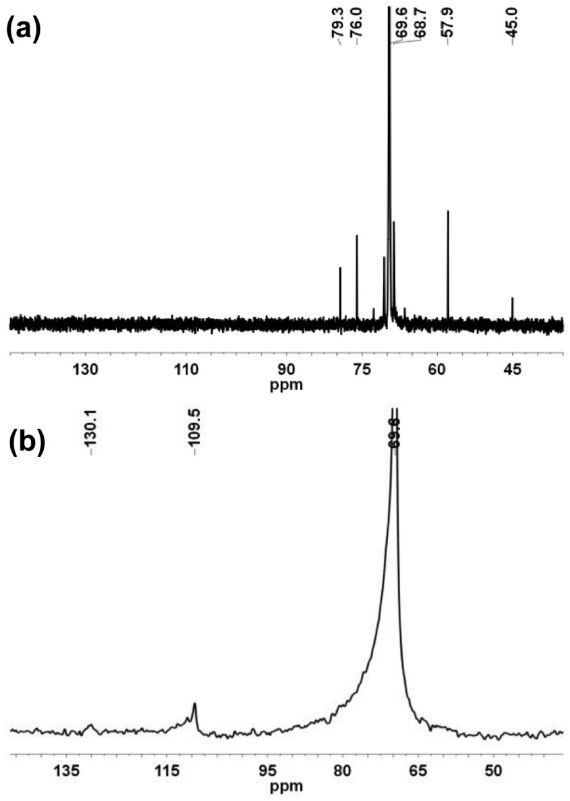

Figure 3. (a) ^{13}C-NMR (400.13 MHz, D_2O) of the PEG-tetraalkyne macromer, (b) ^{13}C MAS NMR (500.13 MHz) spectrum of freeze-dried PEG hydrogel synthesized under photoinitiated cross-linking reactions in the presence of Cu(I), ligand (**L**), and Irgacure 2959.

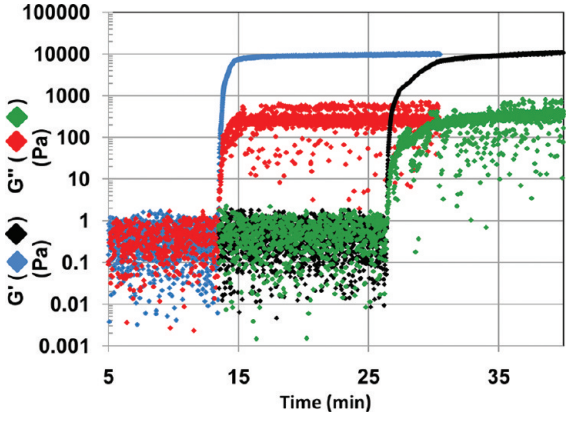

Figure 4. The evolution of the storage (G') and loss moduli (G'') from the photoinitiated cross-linking of PEG-tetraalkyne in the presence and absence of Cu(I) and ligand (**L**): blue and red and black and green, respectively.

Surface Patterning of PEG Hydrogels. Figure 1C and Scheme 1 outlines the procedure for the patterning of PEG hydrogels in a process analogous to photolithography. Surface functionalization of a silicon wafer with a previously reported bromine functionalized plasma polymer (BrPP)[21] was achieved via the radio frequency glow discharge (RFGD) of 1-bromopropane. The bromine groups in the PP undergo nucleophilic exchange with azides (N_3PP), to form a "clickable" surface for the grafting of alkyne-functionalized PEG. An aqueous solution of PEG-tetraalkyne (10 kDa), the photoinitiator, the ligand (**L**), and $CuSO_4{\cdot}5H_2O$ was spin-cast onto

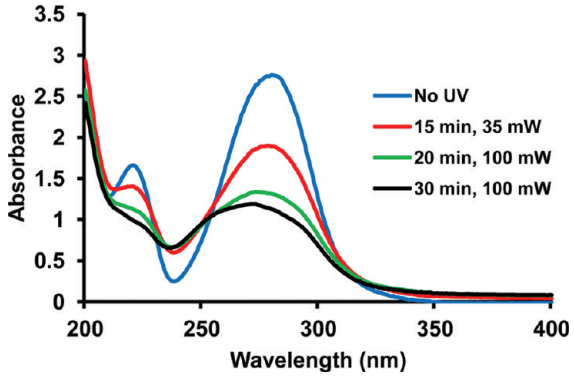

Figure 5. Absorbance spectra of aqueous solutions of Irgacure 2959 after being irradiated with 250−450 nm light at various intensities and durations.

Scheme 1. Schematic Procedure for the Photolithographical Patterning of PEG Hydrogels: (A) Deposition of a BrPP Film Followed by Azide Nucleophilic Exchange Resulting in a N_3PP Film; (B) A Polymer Precursor Solution is Spin-Cast onto the Film; (C) UV Irradiation is Applied through a Photomask; (D) PEG Hydrogel Pattern Is Developed by Rinsing off Unreacted Polymer

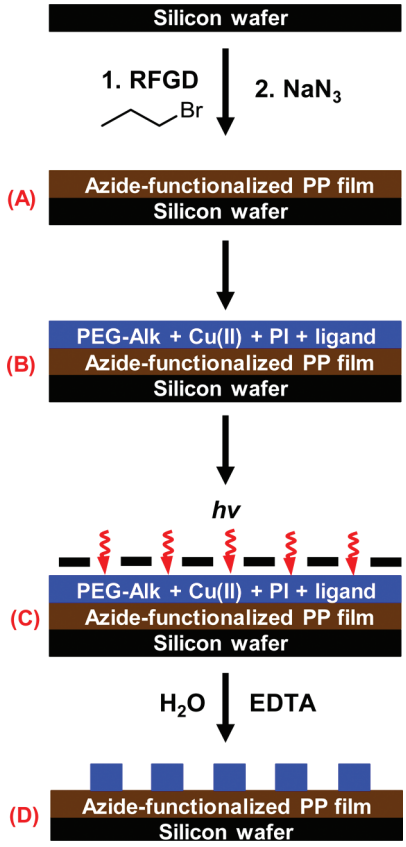

the N_3PP surface with a film thickness of about 1.1 μm, as measured by stylus profilometry (data not shown). A photomask with equidistant 60 μm wide chrome lines (on a quartz plate) was placed in contact with the polymer film and was subsequently irradiated with UV light at room temperature. The spin-cast film behaves as a negative photoresist, where exposed areas undergo photoinitiated click grafting, and cross-linking to form surface grafted hydrogels. The patterns were

dx.doi.org/10.1021/bm201802w | *Biomacromolecules* 2012, 13, 889−895

developed by washing away unreacted polymer in the masked areas with water and ethylenediaminetetraacetic acid solution (EDTA) to remove copper.[27]

Figure 6 shows that the patterns were readily reproduced in the form of PEG hydrogels after just 250 s of UV irradiation.

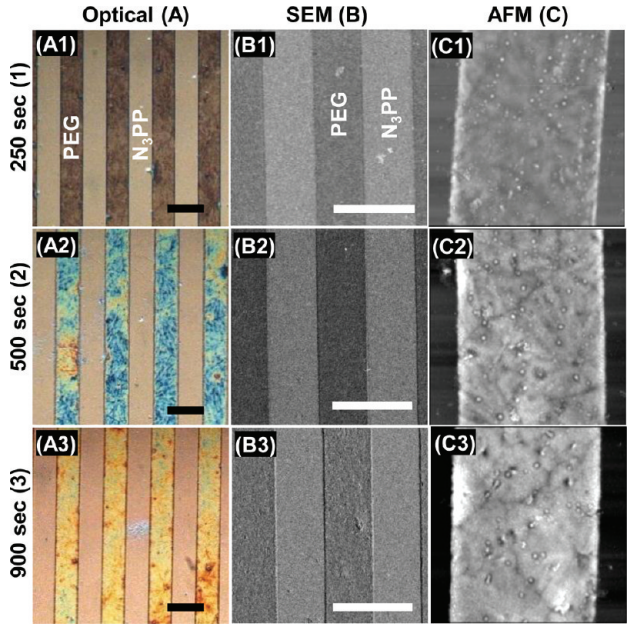

Figure 6. Optical (A), scanning electron microscopy (SEM; B), and atomic force microscopy (AFM; C) images of patterned PEG hydrogels (line width ca. 60 μm) on N_3PP-coated silicon wafers fabricated using three different UV irradiation exposure times. The interference colors of the PEG hydrogels in the optical images are the result of their vastly different thicknesses. Scale bars represent 100 μm. The AFM scan area is 80 × 80 μm with a *z*-height of 400 nm.

The increase in reaction rates when compared to solution-based rheology experiments is a result of the large increase in functional group concentration in the spin-cast film. Well-defined line patterns with minimal residual polymer on the N_3PP film were observed. AFM and SEM analysis revealed that the line features were only about 2−3 μm wider than the mask. This indicates that there is minimal translational diffusion of catalytic Cu(I), which is consistent with observations from Bowman and co-workers.[12a] The presence of the click ligand (**L**) stabilizing Cu(I) is likely to contribute to the decrease in its diffusion. AFM and stylus profilometry analyses also revealed that the thicknesses of the PEG hydrogels (dehydrated) were directly influenced by the UV irradiation time. Thicknesses of about 56 ± 6, 191 ± 12, and 284 ± 10 nm were measured for samples irradiated for 250, 500, and 900 s, respectively (Figure S2a−c). Increasing the irradiation time resulted in a corresponding increase in cross-linking reactions, and thus, a more extensive polymer network was developed. The thickness was also influenced by the molecular weight of the PEG-tetraalkyne. When a 20 kDa PEG was exposed to 500 s of UV irradiation, the thickness of the polymer film was reduced to 117 ± 10 nm (Figure S2d). This is due to the 20 kDa macromer having longer length PEG chains and lower concentrations of cross-linkable alkyne groups, which results in a higher molecular mesh size and a lower cross-link density.[11e,28] The patterned PEG hydrogels were stable and adherent to the surface after autoclaving (10 min, 240 kPa, 121 °C), in contrast to surfaces prepared without azide-functionalization (bare silicon wafers), which resulted in the hydrogels being washed away with water. This confirms that the hydrogels were covalently attached to the surface via the alkyne−azide click reaction. Similarly, control experiments in the absence of either UV light, the photoinitiator, or the click ligand (**L**), did not result in patterned hydrogels after rinsing with water. Interestingly, a control experiment without added Cu(II) in the spin-cast film led to patterned hydrogels, with about 85 μm line features after 500 s of UV irradiation (Figure S3). Analysis by inductively coupled plasma atomic emission spectroscopy (ICP-AES) of the click ligand (**L**) revealed that there was 0.05 mol % of residual copper, presumably remaining following its synthesis by the CuAAC click reaction.[22a] This residual copper was sufficient to catalyze the formation of the PEG hydrogels.

Surface analysis by X-ray photoelectron spectroscopy (XPS) of the PEG hydrogels (dehydrated) revealed only carbon (68.4 ± 0.2%) and oxygen (31.6 ± 0.2%) species with atomic concentrations almost identical to the PEG-tetraalkyne macromer (C: 69 ± 0.2%, O: 31 ± 0.2%) (see Supporting Information, Table S1). The high-resolution C 1s XPS spectrum of the hydrogel displays a broader profile and a greater component contribution around 285 eV compared to the macromer, which is indicative of cross-linking (Figure S6a,g). In the control hydrogel, without the addition of Cu(II), the high resolution C 1s XPS spectrum had a lower component contribution at 285 eV compared to when Cu(II) was added (Figure S6c). This indicates a lower cross-linking density, which contributes to the reduction in thickness and correlates well with the slower gelation kinetics observed in Figure 4.

The attachment of cells on surfaces can be spatially manipulated by the patterning of PEG hydrogels.[11] Figure 7 demonstrates the selective attachment of L929 mouse fibroblast cells onto azide-functionalized bromine plasma polymer films patterned with the PEG hydrogel lines of varying thicknesses. It is clear that the dimensions of the hydrophilic PEG hydrogels, about 60 μm widths with heights over 50 nm, were capable of containing and confining the L929 fibroblast cells to the hydrophobic cell adherent regions (N_3PP film). Cell attachment on the control samples (unpatterned) did not display this selectivity (Figure S4). There was sufficient area in the cell adherent regions for the fibroblast cells to spread and remain viable,[29] as indicated via cellular esterase activity assay with the fibroblast cells being fluorescently labeled with calcein (Figure S5).

The versatility of the patterned surface extends to their spatially resolved chemical functionality. This is particularly useful for the spatial arrangement of biomolecules for targeted and bioresponsive applications. The use of alkyne-functionalized polymers is of benefit due to their ability to be postmodified using click reactions. The residual alkyne groups in the PEG hydrogel and azide groups in the N_3PP regions were selectively labeled with fluorescent dyes using sequential alkyne−azide click reactions. Figure 8 shows that there is minimal cross-contamination between the two areas, with good delineation between the differently functionalized regions.

In conclusion, we have demonstrated the surface patterning of PEG hydrogels via photoinitiated click and radical cross-linking reactions of an alkyne-functionalized PEG on an azide-functionalized surface (N_3PP film). The well-resolved PEG hydrogel patterns were fabricated with thicknesses that are tunable in response to UV exposure time and the molecular

dx.doi.org/10.1021/bm201802w | *Biomacromolecules* 2012, 13, 889−895

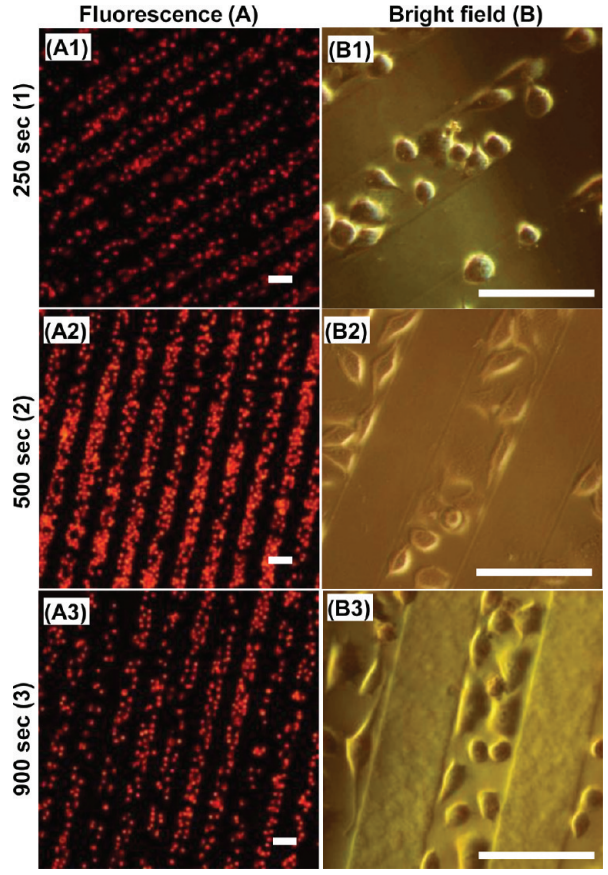

Figure 7. Fluorescence (A1−A3) and bright field (B1−B3) images of patterned PEG hydrogels (line widths ca. 60 μm), prepared at three different UV irradiation exposure times, showing attachment of DilC12(3) stained L929 mouse fibroblast cells at different UV irradiation times. Scale bars represent 100 μm.

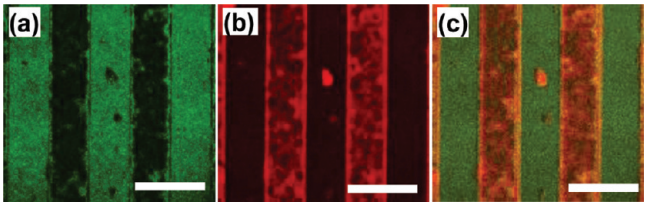

Figure 8. Fluorescence images of patterned PEG hydrogels postfunctionalized by sequential alkyne−azide click reactions (in solution): (a) reaction between azides in the PP with Alexa Fluor (AF) 488-alkyne; (b) reaction between alkynes in the hydrogels with AF-647-azide; (c) overlay of both images. Scale bars represent 100 μm.

weight of the PEG macromer. Surfaces functionalized with these PEG hydrogel patterns resulted in highly functional surfaces, with spatially controlled cell-attachment and chemical functionality. The method is broadly applicable to a wide variety of material surfaces and combines the advantages of click chemistry and photolithography processes. Thus, there is potential for this method to find a range of applications within the fields of biosensors and biomaterials.

■ ASSOCIATED CONTENT

Ⓢ Supporting Information

Details of model compound reactions along with NMR, AFM, XPS, and cell attachment data. This material is available free of charge via the Internet at http://pubs.acs.org.

■ AUTHOR INFORMATION

Corresponding Author

*E-mail: ben.muir@csiro.au.

Notes

The authors declare no competing financial interest.

■ ACKNOWLEDGMENTS

The authors acknowledge Assoc. Prof. J. Forsythe (Monash University) along with Dr. P. Leech and F. Glenn (CSIRO) for their generous gifts of the photoinitiator and the photomask, respectively. We also acknowledge S. M. Pereira (CSIRO) for synthesizing the ligand, A. Balachandra, K. M. Tsang, and Dr. X. Hao (CSIRO) for assistance with rheology, Dr. R. Mulder (CSIRO) for assistance with NMR analysis, Y. Gozukara (CSIRO) for ICP analysis, and Dr. J. Cervenka (University of Melbourne) for Raman analysis. This research was supported by the Australian Research Council under the Federation Fellowship, Discovery Project, and Postdoctoral Fellowship schemes and by CSIRO OCE funding.

■ REFERENCES

(1) (a) Ratner, B. D.; Bryant, S. J. *Annu. Rev. Biomed. Eng.* **2004**, *6*, 41. (b) Rana, D.; Matsuura, T. *Chem. Rev.* **2010**, *110*, 2448.

(2) (a) Banerjee, I.; Pangule, R. C.; Kane, R. S. *Adv. Mater.* **2011**, *23*, 690. (b) Krishnan, S.; Weinman, C. J.; Ober, C. K. *J. Mater. Chem.* **2008**, *18*, 3405. (c) Thissen, H.; Gengenbach, T.; du Toit, R.; Sweeney, D. F.; Kingshott, P.; Griesser, H. J.; Meagher, L. *Biomaterials* **2010**, *31*, 5510.

(3) Prime, K. L.; Whitesides, G. M. *J. Am. Chem. Soc.* **1993**, *115*, 10714.

(4) (a) Hucknall, A.; Rangarajan, S.; Chilkoti, A. *Adv. Mater.* **2009**, *21*, 2441. (b) Kenausis, G. L.; Vörös, J.; Elbert, D. L.; Huang, N.; Hofer, R.; Ruiz-Taylor, L.; Textor, M.; Hubbell, J. A.; Spencer, N. D. *J. Phys. Chem. B* **2000**, *104*, 3298.

(5) (a) Folch, A.; Toner, M. *Annu. Rev. Biomed. Eng.* **2000**, *2*, 227. (b) Nie, Z.; Kumacheva, E. *Nat. Mater.* **2008**, *7*, 277. (c) Falconnet, D.; Csucs, G.; Michelle Grandin, H.; Textor, M. *Biomaterials* **2006**, *27*, 3044. (d) Hook, A. L.; Voelcker, N. H.; Thissen, H. *Acta Biomater.* **2009**, *5*, 2350. (e) Slaughter, B. V.; Khurshid, S. S.; Fisher, O. Z.; Khademhosseini, A.; Peppas, N. A. *Adv. Mater.* **2009**, *21*, 3307. (f) Khademhosseini, A.; Langer, R.; Borenstein, J.; Vacanti, J. P. *Proc. Natl. Acad. Sci. U.S.A.* **2006**, *103*, 2480. (g) Huebsch, N.; Mooney, D. J. *Nature* **2009**, *462*, 426.

(6) Ma, H.; Hyun, J.; Stiller, P.; Chilkoti, A. *Adv. Mater.* **2004**, *16*, 338.

(7) (a) Suh, K.-Y.; Park, M. C.; Kim, P. *Adv. Funct. Mater.* **2009**, *19*, 2699. (b) Suh, K. Y.; Seong, J.; Khademhosseini, A.; Laibinis, P. E.; Langer, R. *Biomaterials* **2004**, *25*, 557. (c) Khademhosseini, A.; Jon, S.; Suh, K. Y.; Tran, T. N. T.; Eng, G.; Yeh, J.; Seong, J.; Langer, R. *Adv. Mater.* **2003**, *15*, 1995. (d) Kim, P.; Kim, D. H.; Kim, B.; Choi, S. K.; Lee, S. H.; Khademhosseini, A.; Langer, R.; Suh, K. Y. *Nanotechnology* **2005**, *16*, 2420.

(8) (a) Falconnet, D.; Koenig, A.; Assi, F.; Textor, M. *Adv. Funct. Mater.* **2004**, *14*, 749. (b) Fan, X.; Lin, L.; Dalsin, J. L.; Messersmith, P. B. *J. Am. Chem. Soc.* **2005**, *127*, 15843.

(9) Menzies, D. J.; Gengenbach, T.; Forsythe, J. S.; Birbilis, N.; Johnson, G.; Charles, C.; McFarland, G.; Williams, R. J.; Fong, C.; Leech, P.; McLean, K.; Muir, B. W. *Chem. Commun* **2012**, *48*, 1907.

(10) Park, E. J.; Carroll, G. T.; Turro, N. J.; Koberstein, J. T. *Soft Matter* **2009**, *5*, 36.

(11) (a) Revzin, A.; Russell, R. J.; Yadavalli, V. K.; Koh, W.-G.; Deister, C.; Hile, D. D.; Mellott, M. B.; Pishko, M. V. *Langmuir* **2001**, *17*, 5440. (b) Revzin, A.; Tompkins, R. G.; Toner, M. *Langmuir* **2003**, *19*, 9855. (c) Koh, W.-G.; Revzin, A.; Simonian, A.; Reeves, T.; Pishko, M. *Biomed. Microdev.* **2003**, *5*, 11. (d) Kloxin, A. M.; Kloxin, C. J.; Bowman, C. N.; Anseth, K. S. *Adv. Mater.* **2010**, *22*, 3484. (e) Ekblad,

T.; et al. *Biomacromolecules* **2008**, *9*, 2775. (f) Hahn, M. S.; Taite, L. J.; Moon, J. J.; Rowland, M. C.; Ruffino, K. A.; West, J. L. *Biomaterials* **2006**, *27*, 2519. (g) Moon, J. J.; Hahn, M. S.; Kim, I.; Nsiah, B. A.; West, J. L. *Tissue Eng., Part A* **2008**, *15*, 579.

(12) (a) Adzima, B. J.; Tao, Y.; Kloxin, C. J.; DeForest, C. A.; Anseth, K. S.; Bowman, C. N. *Nat. Chem* **2011**, *3*, 256. (b) Tasdelen, M. A.; Yagci, Y. *Tetrahedron Lett.* **2010**, *51*, 6945. (c) Tasdelen, M. A.; Yilmaz, G.; Iskin, B.; Yagci, Y. *Macromolecules* **2011**, *45*, 56.

(13) (a) Evans, R. A. *Aust. J. Chem.* **2007**, *60*, 384. (b) Johnson, J. A.; Finn, M. G.; Koberstein, J. T.; Turro, N. J. *Macromol. Rapid Commun.* **2008**, *29*, 1421. (c) Such, G. K.; Quinn, J. F.; Quinn, A.; Tjipto, E.; Caruso, F. *J. Am. Chem. Soc.* **2006**, *128*, 9318.

(14) (a) Hoyle, C. E.; Bowman, C. N. *Angew. Chem., Int. Ed.* **2010**, *49*, 1540. (b) Shah, S. S.; Kim, M.; Cahill-Thompson, K.; Tae, G.; Revzin, A. *Soft Matter* **2011**, *7*, 3133. (c) DeForest, C. A.; Polizzotti, B. D.; Anseth, K. S. *Nat. Mater.* **2009**, *8*, 659. (d) Connal, L. A.; Kinnane, C. R.; Zelikin, A. N.; Caruso, F. *Chem. Mater.* **2009**, *21*, 576. (e) Gupta, N.; Lin, B. F.; Campos, L. M.; Dimitriou, M. D.; Hikita, S. T.; Treat, N. D.; Tirrell, M. V.; Clegg, D. O.; Kramer, E. J.; Hawker, C. J. *Nat. Chem.* **2010**, *2*, 138.

(15) (a) Lowe, A. B.; Hoyle, C. E.; Bowman, C. N. *J. Mater. Chem.* **2010**, *20*, 4745. (b) Hensarling, R. M.; Doughty, V. A.; Chan, J. W.; Patton, D. L. *J. Am. Chem. Soc.* **2009**, *131*, 14673.

(16) (a) Song, W.; Wang, Y.; Qu, J.; Lin, Q. *J. Am. Chem. Soc.* **2008**, *130*, 9654. (b) Song, W.; Wang, Y.; Qu, J.; Madden, M. M.; Lin, Q. *Angew. Chem., Int. Ed.* **2008**, *47*, 2832.

(17) (a) Arumugam, S.; Popik, V. V. *J. Am. Chem. Soc.* **2011**, *133*, 5573. (b) Gruendling, T.; Oehlenschlaeger, K. K.; Frick, E.; Glassner, M.; Schmid, C.; Barner-Kowollik, C. *Macromol. Rapid Commun.* **2011**, *32*, 807.

(18) (a) Tasdelen, M. A.; Uygun, M.; Yagci, Y. *Macromol. Rapid Commun.* **2011**, *32*, 58. (b) Tasdelen, M. A.; Uygun, M.; Yagci, Y. *Macromol. Chem. Phys.* **2010**, *211*, 2271. (c) Tasdelen, M. A.; Uygun, M.; Yagci, Y. *Macromol. Chem. Phys.* **2011**, *212*, 2036.

(19) (a) Doytcheva, M.; Dotcheva, D.; Stamenova, R.; Orahovats, A.; Tsvetanov, C.; Leder, J. *J. Appl. Polym. Sci.* **1997**, *64*, 2299. (b) Doycheva, M.; Petrova, E.; Stamenova, R.; Tsvetanov, C.; Riess, G. *Macromol. Mater. Eng.* **2004**, *289*, 676. (c) Tasdelen, M.; Moszner, N.; Yagci, Y. *Polym. Bull.* **2009**, *63*, 173. (d) Emami, S. H.; Salovey, R.; Hogen-Esch, T. E. *J. Polym. Sci., Part A: Polym. Chem.* **2002**, *40*, 3021.

(20) (a) Carroll, G. T.; Devon Triplett, L.; Moscatelli, A.; Koberstein, J. T.; Turro, N. J. *J. Appl. Polym. Sci.* **2011**, *122*, 168. (b) Spruell, J. M.; Wolffs, M.; Leibfarth, F. A.; Stahl, B. C.; Heo, J.; Connal, L. A.; Hu, J. G.; Hawker, C. J. *J. Am. Chem. Soc.* **2011**, *133*, 16698. (c) Tillet, G.; Boutevin, B.; Ameduri, B. *Prog. Polym. Sci.* **2011**, *36*, 191. (d) Nimmo, C. M.; Shoichet, M. S. *Bioconjugate Chem.* **2011**, *22*, 2199.

(21) (a) Chen, R. T.; Muir, B. W.; Such, G. K.; Postma, A.; Evans, R. A.; Pereira, S. M.; McLean, K. M.; Caruso, F. *Langmuir* **2010**, *26*, 3388. (b) Chen, R. T.; Muir, B. W.; Such, G. K.; Postma, A.; McLean, K. M.; Caruso, F. *Chem. Commun.* **2010**, *46*, 5121. (c) Chen, R. T.; Muir, B. W.; Thomsen, L.; Tadich, A.; Cowie, B. C. C.; Such, G. K.; Postma, A.; McLean, K. M.; Caruso, F. *J. Phys. Chem. B* **2011**, *115*, 6495.

(22) (a) Hong, V.; Udit, A. K.; Evans, R. A.; Finn, M. G. *ChemBioChem* **2008**, *9*, 1481. (b) Kamphuis, M. M. J.; Johnston, A. P. R; Such, G. K.; Dam, H. H.; Evans, R. A.; Scott, A. M.; Nice, E. C.; Heath, J. K.; Caruso, F. *J. Am. Chem. Soc.* **2010**, *132*, 15881.

(23) Beamson, G.; Briggs, H., *High Resolution XPS of Organic Polymers: The Scienta ESCA300 Database*; John Wiley and Sons: Chichester, U.K., 1992.

(24) (a) Chan, T. R.; Hilgraf, R.; Sharpless, K. B.; Fokin, V. V. *Org. Lett.* **2004**, *6*, 2853. (b) Rodionov, V. O.; Presolski, S. I.; Gardinier, S.; Lim, Y.-H.; Finn, M. G. *J. Am. Chem. Soc.* **2007**, *129*, 12696.

(25) (a) Wu, W.; Parent, J. S. *J. Polym. Sci., Part A: Polym. Chem.* **2008**, *46*, 7386. (b) Chen, Z.; Zhang, Y.-X.; An, Y.; Song, X.-L.; Wang, Y.-H.; Zhu, L.-L.; Guo, L. *Eur. J. Org. Chem.* **2009**, *2009*, 5146.

(26) Hein, J. E.; Fokin, V. V. *Chem. Soc. Rev.* **2010**, *39*, 1302.

(27) Malkoch, M.; Vestberg, R.; Gupta, N.; Mespouille, L.; Dubois, P.; Mason, A. F.; Hedrick, J. L.; Liao, Q.; Frank, C. W.; Kingsbury, K.; Hawker, C. J. *Chem. Commun.* **2006**, 2774.

(28) Lin-Gibson, S.; Jones, R. L.; Washburn, N. R.; Horkay, F. *Macromolecules* **2005**, *38*, 2897.

(29) Chen, C. S.; Mrksich, M.; Huang, S.; Whitesides, G. M.; Ingber, D. E. *Biotechnol. Prog.* **1998**, *14*, 356.